

# Single C-Reactive Protein Molecule Detection on a Gold-Nanopatterned Chip Based on Total Internal Reflection Fluorescence

Yunmi Heo, Seungah Lee, Sang-Won Lee,<sup>†</sup> and Seong Ho Kang<sup>\*</sup>

Department of Applied Chemistry, College of Applied Science, Kyung Hee University, Yongin-si, Gyeonggi-do 446-701, Korea  
<sup>\*</sup>E-mail: shkang@khu.ac.kr

<sup>†</sup>Department of Plant Molecular Systems, Biotechnology & Crop Biotech Institute, Kyung Hee University,  
Yongin-si, Gyeonggi-do 446-701, Korea

Received May 18, 2013, Accepted June 22, 2013

Single C-reactive protein (CRP) molecules, which are non-specific acute phase markers and products of the innate immune system, were quantitatively detected on a gold-nanopatterned biochip using evanescent field-enhanced fluorescence imaging. The  $4 \times 5$  gold-nanopatterned biochip (spot diameter of 500 nm) was fabricated by electron beam nanolithography. Unlabeled CRP molecules in human serum were identified with single-molecule sandwich immunoassay by detecting secondary fluorescence generated by total internal reflection fluorescence (TIRF) microscopy. With decreased standard CRP concentrations, relative fluorescence intensities reduced in the range of 33.3 zM–800 pM. To enhance fluorescence intensities in TIRF images, the distance between biochip surface and CRP molecules was optimally adjusted by considering the quenching effect of gold and the evanescent field intensity. As a result, TIRF only detected one single-CRP molecule on the biochip the first time.

**Key Words :** C-reactive protein, Gold nanoarray chip, Single-molecule detection, Total internal reflection fluorescence (TIRF)

## Introduction

C-reactive protein (CRP), which is composed of five identically arranged 32-kDa protomers, was discovered in 1930.<sup>1,2</sup> CRP is the first acute-phase protein exclusively synthesized by hepatocytes, the main type of liver cell.<sup>3</sup> In human serum, CRP levels increase up to 1000-fold in response to chemical cytokines as an acute-phase response.<sup>4</sup> CRP is well known as a sensitive marker of inflammation, tissue damage, infection, cell necrosis, and some malignancies.<sup>4,6</sup> Increased CRP is also observed after surgical procedures.<sup>7</sup> Elevated serum CRP concentration is associated with cardiovascular diseases, such as heart attack, ischemic stroke, and peripheral arterial disease.<sup>8</sup> As a result, high sensitivity CRP (hs CRP) is an established indicator for heart disease risk.<sup>2</sup> A CRP concentration of 3–10 mg/L (26–90 nM) is considered high risk, 1–3 mg/L (9–26 nM) is considered intermediate risk, and less than 1 mg/L (9 nM) is considered low risk.<sup>7</sup>

Conventional enzyme-linked immunosorbent assay (ELISA) has been widely used to detect CRP molecules.<sup>9,10</sup> Other analytical methods have been used for this purpose in the last few years, including radial immunodiffusion, electroimmunoassay, immunoturbidimetry, laser nephelometry,<sup>11</sup> immunoradiometric assay,<sup>12</sup> fluorescence-based immunochromatographic method,<sup>13</sup> and time-resolved immunofluorometric assay.<sup>14</sup> New techniques have recently been developed, such as electrochemical immunoassay,<sup>15</sup> electrochemiluminoimmunoassay,<sup>16</sup> electrochemical impedance immunosensor,<sup>17</sup> immunoassay based on magnetic nanoparticles,<sup>18</sup>

spectral surface plasmon resonance biosensor,<sup>19</sup> immunochromatographic assay,<sup>20</sup> lateral flow assay,<sup>21</sup> and microfluidic electrochemical sensor.<sup>22</sup> Furthermore, the feasibility of using microarray biochips to analyze cytokines in serum samples has been reported<sup>23,24</sup> and proven highly reliable. However, these techniques are relatively expensive and not sensitive enough to identify specific target molecules at ultra-low concentration. In addition, they require relatively long incubation times and large amounts of samples and reactants.<sup>25–27</sup> The nanoarray biochip method has begun to emerge as a potential route for overcoming the above problems. Biochip miniaturization was enabled with developments in dip-pen nanolithography,<sup>28</sup> ink-jet printing,<sup>29</sup> and electrospray deposition.<sup>30</sup> More recently, protein molecules were detected at the zeptomolar concentration level (zM,  $\times 10^{-21}$  M) using a mass spectrometer, gold nanoparticles or fluorescent dye conjugated with antibodies.<sup>31–34</sup> Although target molecules and antibodies form specific complexes that can emit signals, the identification of proteins in the zM concentration is still difficult to achieve. There are theoretically very few molecules in the zM range, so the signal is weak or invisible.

In this work, a single-molecule sandwich immunoassay based on a gold-nanopatterned biochip was developed for quantitative analysis of acute phase cytokines at extremely low concentrations in serum samples. Molecules of target protein were visualized as fluorescence using a total internal reflection fluorescence (TIRF) system based on evanescent field fluorescence intensity imaging. To enhance fluorescence intensities more than those of previous reports using nano-

array biochips,<sup>33,34</sup> the distance between the glass biochip substrate and the fluorescence dye was optimally adjusted. This enabled maximum evanescent field intensities while minimizing the quenching effect of gold. In addition, a gold-patterning spot with a diameter of 500 nm was used to increase the opportunities to bind scarce target molecules with fixed primary antibodies. Because of the high sensitivity achieved in this study, wide-range quantification of CRP was possible. Low concentration proteins were detected at single molecule levels. Furthermore, one individual CRP molecule was detected at 33.3 zM concentration.

## Experimental

**Reagents Preparation.** A 4-inch soda-lime glass wafer was purchased from Winwin Tech (Bucheon-si, Korea). Dithiobis (succinimidyl propionate) (DSP) and Protein A/G were purchased from Pierce (Rockford, IL, USA). Dimethyl sulfoxide (DMSO) and glycine were purchased from Sigma-Aldrich Inc. (St. Louis, MO, USA). Tris(Base) was purchased from Mallinckrodt Baker, Inc. (Phillipsburg, NJ, USA). StabilGuard was purchased from SurModics (Eden Prairie, MN, USA). Human/mouse/porcine CRP monoclonal antibody, recombinant human CRP, and CRP biotin affinity purified polyclonal antibody were purchased from R&D systems (Minneapolis, MN, USA). Streptavidin-Alexa Fluor<sup>®</sup>488 was from Molecular Probes (Eugene, OR, USA). All solutions were diluted with 1× phosphate buffered saline (PBS, pH 7.4; 137 mM NaCl, 2.7 mM KCl, 4.3 mM Na<sub>2</sub>HPO<sub>4</sub>, 1.4 mM KH<sub>2</sub>PO<sub>4</sub>). The buffers were made of ultra-pure water (> 18 MΩ), filtered with a 0.2 μm membrane filter (Whatman International Ltd., Maidstone, England), and photobleached overnight using a UV-B lamp (G15TE, Philips, The Netherlands).

**Preparation of Gold-Nanopatterned CRP Chip.** The

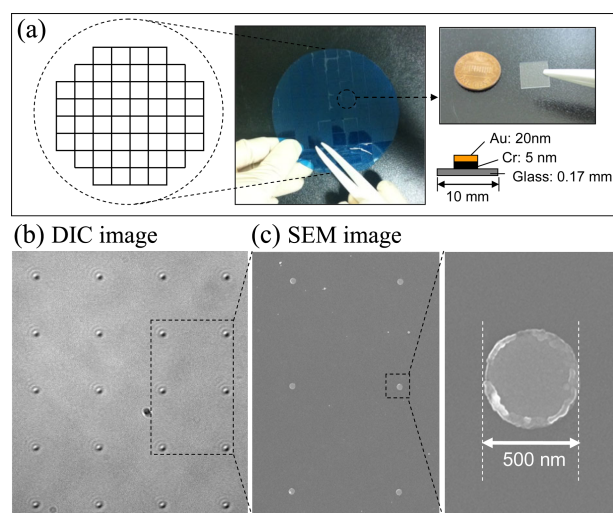


**Figure 1.** (a) Design of the  $4 \times 5$  nanopatterned gold array on the glass substrate, (b) differential interference contrast (DIC) image of  $4 \times 5$  gold-nanopatterned array with spot diameter of 500 nm, (c) scanning electron microscopy (SEM) image of  $2 \times 3$  patterning of gold array and individual gold array spot.

gold-nanopatterned substrate was arranged like those shown in Figure 1 and then fabricated by the National Nanofab Center (Daejeon, South Korea). An electron beam evaporator was used to fabricate a  $4 \times 5$  gold-nanopatterned array containing 500 nm diameter spots with a 10 μm pitch on a 10 mm<sup>2</sup> glass wafer. To enable gold to easily adhere to the glass wafer, substrates were deposited with a 5 nm adhesive layer of chromium at a rate 0.1 nm/s. A 20 nm layer of gold was then coated over the chromium layer at a rate of 0.1 nm/s. Before linker deposition, the chips were prewashed. Chips were immersed in acetone (99.5% purity) for 30 s, and immediately exposed to isopropanol (99.9% purity) for 30 s. The gold-nanopatterned array chips were soaked in piranha

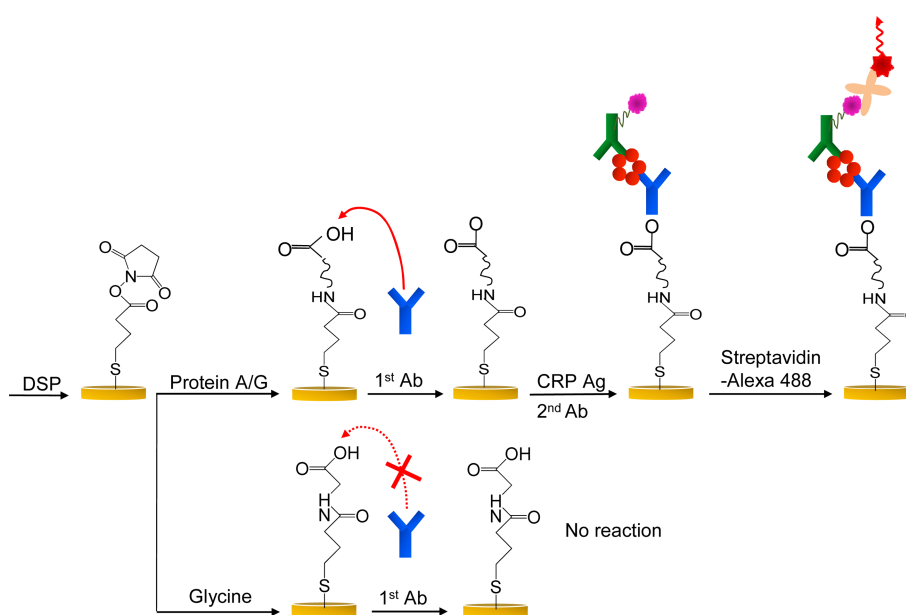


**Figure 2.** Serial procedures for sandwich fluorescence immunoassay on gold-nanopatterned chips. DSP, dithiobis(succinimidyl propionate); Ab, antibody; Ag, antigen.

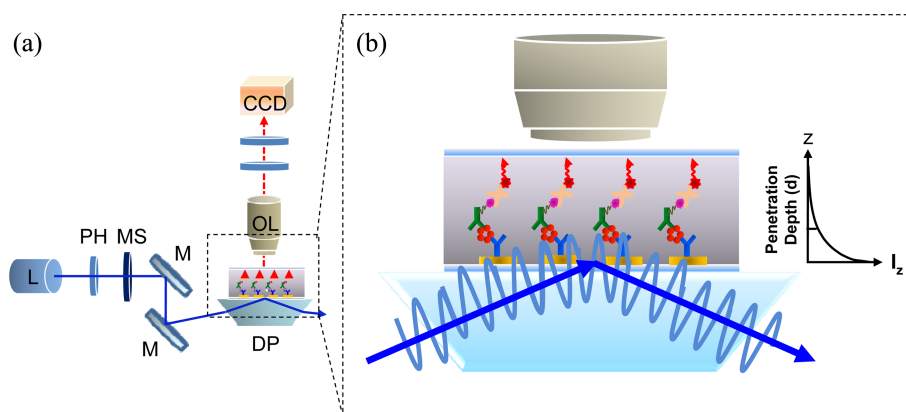


**Figure 3.** (a) Schematic diagram of mechanical setup of lab-made prism-type TIRF system. (b) With total internal reflection, effect of sinusoidal light waves on the gold-nanopatterned chip and graph of evanescent field intensity ( $I_z$ ) with perpendicular distance ( $z$ ). L, laser; PH, pinhole; MS, mechanical shutter; M, mirror; DP, dove prism; OL, objective lens; CCD, charge coupled device.

solution (1:1 =  $\text{H}_2\text{SO}_4$ :30%  $\text{H}_2\text{O}_2$ ) for 30 min and rinsed with distilled water. The washed chips were dried under a stream of nitrogen and stored in a desiccator before use.

**Single CRP Molecule Sandwich Immunoassay on Gold-Nanopatterned Chip.** A series of CRP sandwich immunoassay procedures were conducted,<sup>35</sup> as schematically illustrated in Figure 2. The gold-nanopatterned chips were immersed in 4 mg/mL DSP in DMSO for 30 min and then rinsed with pure DMSO and distilled water. For 1 h, 0.1 mg/mL Protein A/G in PBS was added to the activated gold surface, which was formed by thiolation reaction between the substrates and DSP. Protein A/G was used as a binding material in the sandwich immunoassay because it can bind to the heavy chains of the antibody Fc region. Unreacted succinimide groups were blocked with 10 mM Tris (pH 7.5) and 1 M glycine for 30 min. To stabilize bound proteins, the gold array chips were incubated with StabilGuard for 30 min and rinsed briefly with distilled water. The chips were then incubated with 20  $\mu\text{L}$  of 2  $\mu\text{g}/\text{mL}$  human/mouse/porcine CRP monoclonal antibody (primary antibody) in PBS (pH 7.4) for 1 h. After briefly washing, various concentrations of CRP standard protein were incubated on chips for 1 h. The incubation time of the sample with zM CRP level concentrations was increased to 4 h to allow sufficient time for Brownian motion. Reaction with 20  $\mu\text{L}$  of 2  $\mu\text{g}/\text{mL}$  CRP biotin affinity purified polyclonal antibody (secondary antibody) occurred for 1 h. Twenty  $\mu\text{L}$  of 2  $\mu\text{g}/\text{mL}$  Streptavidin-Alexa Fluor<sup>®</sup>488 was added to the chips and incubated for 30 min to identify fluorescence intensities. CRP concentration was calculated using the TIRF intensity, which was generated by fluorophores in evanescent fields. Chips were washed by soaking in 100 mL  $1\times$  PBS for 2 min and rinsing with distilled water at each step. All reactions were conducted with agitation at room temperature.

**Lab-Made Prism-Type TIRF System.** A diagram of the basic TIRF system is schematically shown in Figure 3(a). The experimental set-up of the lab-made prism-type TIRF system used to detect fluorescence intensity formed by antigen-antibody interactions on the nanopatterned chip was similar to that mentioned in previous reports.<sup>36,37</sup> TIRF was

operated using an upright Olympus BX51 microscope (Olympus Optical Co. Ltd., Tokyo, Japan) with an Olympus 100 $\times$  UPLEL objective lens (oil type, 1.3 N.A., W.D. 0.1 mm). Immersion oil (Immersol<sup>™</sup> 518F, Zeiss,  $n = 1.518$ ) with a similar reflective index to that of the glass slide was used to minimize light refraction. A charge coupled device (CCD) camera (QuantEM 512SC, Photometrics, Tucson, AZ, USA) with an exposure time of 100 ms was used to capture the TIRF images. A Uniblitz mechanical shutter (Vincent Associates, Rochester, NY, USA) was used to lessen the intensity loss caused by photobleaching. A 488 nm notch filter (Korea Electro Optics, Korea) and a 520/10 nm bandpass filter (Semrock, Rochester, NY, USA) were placed between the objective lens and the CCD camera. To carry out TIRF microscopy, the nanopatterned CRP chip was positioned on a transmitted all-side polished dove-type prism with an anti-reflective coating (BK7, 15 mm  $\times$  63 mm  $\times$  15 mm,  $n = 1.522$ , Korea Electro-Optics Co., Ltd., Korea). The laser beam directly entered the prism at the interface between the protein chip and media. It reflected back into the protein chip (total internal reflection) at an incidence angle ( $\theta$ ) slightly greater than  $61.2^\circ$ . All images were acquired and processed using MetaMorph 7.0 software (Universal Imaging Co., Downing Town, PA, USA).

## Results and Discussion

**Detection of Single CRP Molecule via Sandwich Immunoassay on Nanoarray Chip.** While detecting CRP molecules based on single-molecule sandwich fluorescence immunoassay, the fluorescence intensity of the spot rose depending on standard CRP concentrations. As standard CRP concentration increased, the relative fluorescence intensity (RFI) became stronger and the spot size increased (Figure 4). After the gold-nanopatterned chip was stabilized by reaction with StabilGuard for 30 min, it was reacted with primary antibody for 1 h. The chips were then incubated with standard CRP or human serum sample including CRP antigen. Provided that concentrations of CRP antigen were more than 800 zM, the incubation time for primary antibody and CRP

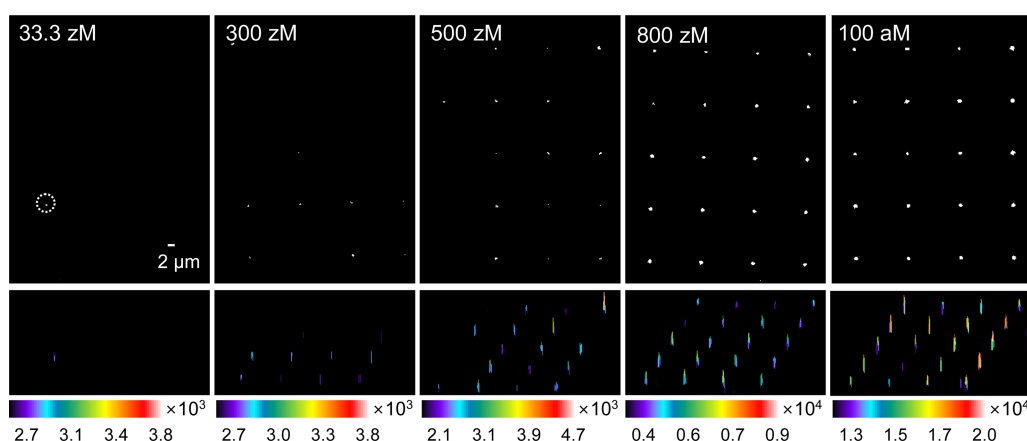


**Figure 4.** Total internal reflection fluorescence imaging of CRP molecules at sub-attomolar (zM) level.

antigen was 1 h and antigen volume was 20  $\mu\text{L}$ . At CRP concentration below 500 zM, the optimum incubation time increased from 1 h to 4 h and antigen volume increased up to 50  $\mu\text{L}$  due to the rareness number of antigen molecules. With a CRP antigen concentration of 500 zM, the theoretical molecule number was only 15. To provide a sufficient molecule number and enough reaction time between the primary antibody and CRP antigen, increases in incubation time and sample volume were required. Under these conditions, a theoretical molecule was computed at 33.3 zM CRP concentration (Table 1). This result indicates that it is possible to detect one single CRP molecule. Although 50 zM CRP was detected on a 3-mercaptopropyl trimethoxysilane-coated cover glass in a previous report,<sup>34</sup> there were problems regarding spot size reproducibility and shelf-life limits. This study achieved the detection of one single CRP molecule on a gold-nanopatterned biochip. The analysis technique of single-molecule sandwich immunoassay on a gold-nanopatterned protein chip could be applied in proteomics and pharmaceuticals to identify single protein molecules.

**Effects of Evanescent Field Intensity and Quenching on Sandwich Immunoassay Imaging.** In the sandwich immunoassay approach based on TIRF, spot RFI was largely determined by evanescent field intensity and the quenching effect of the dye. Evanescent field intensity also had a strong effect on detecting single CRP molecules. The evanescent field intensity was considered depending on distance from the surface (Figure 3(b)). When the incident angle was greater than the critical angle and the refractive index of the incidence medium was larger than that of the aqueous (specimen) medium, total internal reflection was observed near the interface between the two media. In this case, the evanescent field was formed. Although all light was reflected back, an infinitesimal fraction passes through the interface because light waves are sinusoidal. The penetrated light propagated parallel to the interface and produced an evanescent field. With increased perpendicular distance ( $z$ ) from the interface, evanescent field intensity decreased exponentially by:

$$I_z = I_0 e^{-\frac{z}{d}}$$

**Table 1.** Comparison of RFI values with standard CRP concentrations and theoretical molecule numbers

CRP Conc.	Theoretical Mol. No.	RFI <sup>a</sup> ( $\times 10^3$ )
0 zM	0	0
25 zM	0.75	0
33.3 zM	1.00	6.36 $\pm$ 0.1
300 zM	9.03	12.19 $\pm$ 0.5
500 zM	15.05	14.56 $\pm$ 0.3
800 zM	24.08	18.16 $\pm$ 1.5
100 aM	1.20 $\times 10^3$	25.53 $\pm$ 2.1
100 fM	1.20 $\times 10^6$	62.86 $\pm$ 3.4
500 fM	6.02 $\times 10^6$	70.09 $\pm$ 3.8
100 pM	1.20 $\times 10^9$	83.37 $\pm$ 4.4
800 pM	9.63 $\times 10^9$	88.35 $\pm$ 8.8

<sup>a</sup>RFI: relative fluorescence intensity. RFI values were determined by subtracting background intensities from total internal reflection fluorescence intensities.

where  $I_0$  is evanescent field intensity at  $z = 0$ . The penetration depth ( $d$ ) at  $\lambda_0$  was expressed by:

$$d = \frac{\lambda_0}{4\pi\sqrt{n_1^2 \sin^2 \theta - n_2^2}}$$

Penetration depth usually ranged between 30 and 300 nm depending on the refractive indices of the media and independent of the polarization direction of incident light. The penetration depth was similar to or slightly smaller than incident wavelength.

The aqueous area was generated by loading a 1  $\mu\text{L}$  volume of 1 $\times$  PBS buffer between a cover glass and the gold-nanopatterned biochip. Solution thickness was approximately 10  $\mu\text{m}$ . The gold spot of the biochip consisted of a 5 nm adhesive layer of chromium followed by a 20 nm gold layer. The height of the space generated by the reaction between gold array and DSP was 1.2 nm. Protein A/G consisted of Protein A (5 nm) and Protein G (1.35 nm), and contained four Fc binding regions.<sup>38,39</sup> Generally, Y-shaped IgG molecules that were 14.5 nm in height, 4.0 nm in thickness, and 8.5 nm in width were used as primary and secondary antibodies.<sup>40</sup> Streptavidin was 5 nm high.<sup>41</sup> The theoretical distance

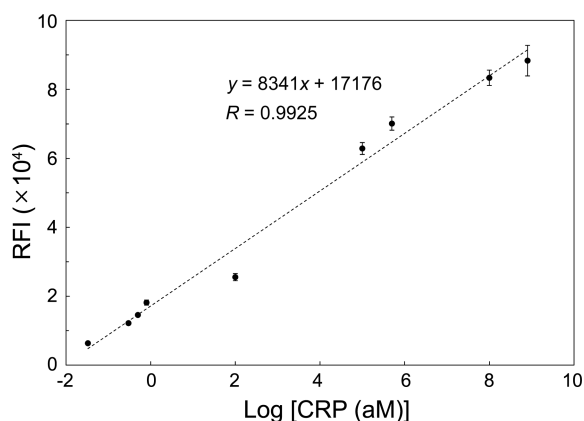


**Figure 5.** Calibration curve of the linear range of standard CRP produced by serial dilutions from 33.3 zM to 800 pM ( $n = 6$ ). Relative fluorescence intensities were corrected by background subtraction.

from the glass substrate surface arrayed gold-patterned spot to the Streptavidin-Alexa Fluor<sup>®</sup>488 was approximately 61.5–65.2 nm. This value indicates that the fluorophores (Alexa Fluor<sup>®</sup>488) were not totally affected by gold quenching. A weakness in fluorescence intensity was observed in the metal surface. Such fluorescence enhancement has been observed when fluorescence dye was placed further than 10 nm from the metal surface.<sup>42,43</sup>

As evanescent field intensity decayed exponentially with increasing vertical distance, the distance between the interface and fluorescence dye shortened as much as possible. The distance had to be further than 10 nm to reduce the gold quenching effect. The theoretical distance of dye from the cover glass of the gold-patterned array chip was shorter than that of a previous report. As a result, the evanescent field intensity was stronger. Therefore, individual CRP molecules were identified more clearly.

**Wide-Range Quantitative CRP Analysis.** Under optimum conditions, quantitative analysis of CRP was possible in the wide range (Figure 5). To draw a calibration curve, standard CRP antigens were serially diluted with  $1\times$  PBS buffer. The linear range of CRP was 33.3 zM to 800 pM (linear regression equation,  $y = 8341x + 17176$ ,  $R = 0.9925$ ) in the sandwich nanoarray biochip immunoassay. When the assay was carried out under a concentration of 33.3 zM or without any CRP standards, no fluorescence spots were identified on TIRF images. RFI was calculated by subtracting spot intensity from background intensity. In this case, spot fluorescence intensity was equivalent to background fluorescence intensity. As a result, the RFI was zero or even negative. Therefore, the LOD was determined to be 33.3 zM in the single-molecule sandwich immunoassay. It means that can be critical role to prevent diseases in preventive medicine or preventive care field.

## Conclusion

We developed a single-molecule sandwich immunoassay based on evanescent field-enhanced fluorescence imaging

on 500 nm gold-nanopatterned biochips. This technique was highly sensitive for CRP detection, and CRP molecules were quantitatively analyzed in a wide range from zM to pM levels. Based on a single-molecule sandwich assay, fluorescence intensities at ultra-low CRP concentrations were observed on TIRF images. The linear response range for the CRP concentration assay was 33.3 zM to 800 pM with a correlation coefficient of 0.9925. The gold nanoarray biochip exhibited a low LOD of 33.3 zM, and only one CRP molecule was observed on the chip. Compared to other previously reported methods, the results of this study were significant for two reasons: (1) This study demonstrated the possibility of studying *in vivo* chemical and physiologic mechanisms of individual protein dynamics, translation, and protein-protein interaction at the single-molecule level. (2) These results are important when studying various physiologic mechanisms at the single-molecule level. In addition, it can be applied for clinical diagnosis of diseases related to high CRP due to high sensitivity in a wide dynamic linear range. This method can also be used to detect poisonous substances that are lethal in small amounts.

**Acknowledgments.** This research was supported by the Bio & Medical Technology Development Program of the National Research Foundation (NRF) funded by the Ministry of Education, Science and Technology (2012-0001130).

## References

- Thompson, D.; Pepys, M. B. *Structure Fold Des.* **1999**, *7*, 169.
- Albrecht, C.; Kaepfel, N.; Gauglitz, G. *Anal. Bioanal. Chem.* **2008**, *391*, 1845.
- Pepys, M. B.; Hirschfield, G. M. *J. Clin. Invest.* **2003**, *111*, 1805.
- Casamassima, A.; Picciariello, M.; Quaranta, M.; Bernardino, R.; Ranieri, C.; Paradiso, A.; Lorusso, V.; Guida, M. *J. Urol.* **2005**, *173*, 52.
- George, S.; Bukowski, R. M. *Cancer* **2008**, *113*, 450.
- Pepys, M. B.; Baltz, M. L. *Adv. Immunol.* **1983**, *34*, 141.
- Pfützner, A.; Forst, T. *Diabetes Technol. Ther.* **2006**, *8*, 28.
- Rifai, N.; Ridker, P. M. *Curr. Opin. Lipidol.* **2002**, *13*, 383.
- Lequin, R. M. *Clin. Chem.* **2005**, *51*, 2415.
- Price, P. C. *Clin. Chem. Lab. Med.* **1998**, *36*, 341.
- Grutzmeier, S.; Schenck, H. V. *Clin. Chem.* **1989**, *35*, 3461.
- Hutchinson, W. L.; Koening, W.; Frohlich, M.; Sund, M.; Lewe, G. D. O.; Pepys, M. B. *Clin. Chem.* **2000**, *46*, 934.
- Oh, S. W.; Moon, J. D.; Park, S. Y.; Jang, H. J.; Kim, J. H.; Nahm, K. B.; Choi, E. Y. *Clin. Chem. Acta* **2005**, *356*, 172.
- Parra, M. D.; Tecles, F.; Suibiela, S. M.; Ceron, J. J. *J. Veterinary Diagnostic Investigation* **2005**, *17*, 139.
- Zhou, F.; Lu, M.; Wang, W.; Bian, Z. P.; Zhang, J. R.; Zhu, J. J. *Clin. Chem.* **2010**, *56*, 1701.
- Kleme, T. A.; Makinen, P.; Ylino, T.; Vare, L.; Kulmala, S.; Ihalainen, P.; Peltonen, J. *Anal. Chem.* **2006**, *78*, 82.
- Chen, X.; Wang, Y.; Zhou, J.; Yan, W.; Li, X.; Zhu, J. J. *Anal. Chem.* **2008**, *80*, 2133.
- Tsai, H. Y.; Hsu, C. F.; Chiu, I. W.; Borfuh, C. *Anal. Chem.* **2007**, *79*, 8416.
- Jung, S. H.; Jung, J. W.; Suh, I. B.; Yuk, J. S.; Kim, W. J.; Choi, E. Y.; Kim, Y. M.; Ha, K. S. *Anal. Chem.* **2007**, *79*, 5703.
- Zhou, G.; Mao, X.; Juncker, D. *Anal. Chem.* **2012**, *84*, 7736.
- Swanson, C.; D'Andrea, A. *Clin. Chem.* **2013**, *59*, 641.
- Dykstra, P. H.; Roy, V.; Byrd, C.; Bentley, W. E.; Ghodssi, R.

- Anal. Chem.* **2011**, 83, 5920.
23. Du, W.; Xu, Z.; Ma, X.; Song, L.; Schneider, E. M. *J. Biotechnol.* **2003**, 106, 87.
24. Andresen, H.; Grotzinger, C.; Zarse, K.; Birringer, M.; Hesseus, C.; Kreuzer, O. J.; Ehrentreich-Forster, E.; Bier, F. F. *Sens. Actuators B: Chem.* **2006**, 113, 655.
25. Henry, J.; Anand, A.; Chowdhury, M.; Cotei, G.; Moreira, R.; Good, T. *Anal. Biochem.* **2004**, 334, 1.
26. Wang, S.; Zhang, C.; Wang, J.; Zhang, Y. *Anal. Chim. Acta* **2005**, 546, 161.
27. Russo, G.; Zegar, C.; Giordan, A. *Oncogene* **2003**, 23, 6497.
28. Lee, K. B.; Park, S. J.; Mirkin, C. A.; Smith, J. C.; Mrksich, M. *Science* **2002**, 295, 1702.
29. Martin, B. D.; Gaber, B. P.; Patterson, C. H.; Turner, D. C. *Langmuir* **1998**, 14, 3971.
30. Morozov, V. N.; Morozova, T. Y. *Anal. Chem.* **1999**, 71, 1415.
31. Hou, S. Y.; Chen, H. K.; Cheng, H. C.; Huang, C. Y. *Anal. Chem.* **2007**, 79, 980.
32. Shen, Y.; Tolic, N.; Masselon, C.; Pasa-Tolic, L.; Camp, D. G.; Lipton, M. S.; Anderson, G. A.; Smith, R. D. *Anal. Bioanal. Chem.* **2004**, 387, 1037.
33. Lee, S.; Lee, S.; Ko, Y. H.; Jung, H.; Kim, J. D.; Song, J. M.; Choo, J.; Eo, S. K.; Kang, S. H. *Talanta* **2009**, 78, 608.
34. Islam, S.; Lee, H. G.; Choo, J.; Song, J. M.; Kang, S. H. *Talanta* **2010**, 81, 1402.
35. Lee, K.; Lee, S.; Yu, H.; Kang, S. H. *J. Nanosci. Nanotechnol.* **2010**, 10, 3228.
36. Lee, S.; Choi, J. S.; Kang, S. H. *J. Nanosci. Nanotechnol.* **2007**, 7, 3689.
37. Kang, S. H.; Kim, Y. J.; Yeung, E. S. *Anal. Bioanal. Chem.* **2007**, 387, 2663.
38. Bjork, I. *Eur. J. Biochem.* **1972**, 29, 579.
39. Lee, J. M.; Park, H. K.; Jung, Y.; Kim, J. K.; Jung, S. O.; Chung, B. H. *Anal. Chem.* **2007**, 79, 2680.
40. Lynch, M.; Mosher, C.; Huff, J.; Nettikadan, S.; Johnson, J.; Henderson, E. *Proteomics* **2004**, 4, 1695.
41. Anderson, A. S.; Dattelbaum, A. M.; Montano, G. A.; Price, D. N.; Schmidt, J. G.; Martinez, J. S.; Grace, W. K.; Grace, K. M.; Swanson, B. I. *Langmuir* **2008**, 24, 2240.
42. Stefani, F.; Gerbeth, G. *Phys. Rev. Lett.* **2005**, 94, 023005/1-023005/4.
43. Lakowicz, J. R.; Malicka, J.; D'Auria, S.; Gryczynski, I. *Anal. Biochem.* **2003**, 320, 13.
-